ORIGINAL RESEARCH

Inhibition of Vascular c-Jun N-Terminal Kinase 2 Improves Obesity-Induced Endothelial Dysfunction After Roux-en-Y Gastric Bypass

Petia Doytcheva, PhD; Thomas Bächler, MD; Erika Tarasco, MSc; Vincenzo Marzolla, PhD; Michael Engeli, MSc; Giovanni Pellegrini, DVM, PhD; Simona Stivala, PhD; Lucia Rohrer, PhD; Francesco Tona, MD, PhD; Giovanni G. Camici, PhD; Paul M. Vanhoutte, MD, PhD; Christian M. Matter, MD; Thomas A. Lutz, DVM, PhD; Thomas F. Lüscher, MD; Elena Osto, MD, PhD

***Background*—**Roux-en-Y gastric bypass (RYGB) reduces obesity-associated comorbidities and cardiovascular mortality. RYGB improves endothelial dysfunction, reducing c-Jun N-terminal kinase (JNK) vascular phosphorylation. JNK activation links obesity with insulin resistance and endothelial dysfunction. Herein, we examined whether JNK1 or JNK2 mediates obesity-induced endothelial dysfunction and if pharmacological JNK inhibition can mimic RYGB vascular benefits.

***Methods and Results*—**After 7 weeks of a high-fat high-cholesterol diet, obese rats underwent RYGB or sham surgery; sham–operated ad libitum–fed rats received, for 8 days, either the control peptide D-TAT or the JNK peptide inhibitor D-JNKi-1 (20 mg/kg per day subcutaneous). JNK peptide inhibitor D-JNKi-1 treatment improved endothelial vasorelaxation in response to insulin and glucagon-like peptide-1, as observed after RYGB. Obesity increased aortic phosphorylation of JNK2, but not of JNK1. RYGB and JNK peptide inhibitor D-JNKi-1 treatment blunted aortic JNK2 phosphorylation via activation of glucagon-like peptide-1–mediated signaling. The inhibitory phosphorylation of insulin receptor substrate-1 was reduced, whereas the protein kinase B/endothelial NO synthase pathway was increased and oxidative stress was decreased, resulting in improved vascular NO bioavailability.

***Conclusions*—**Decreased aortic JNK2 phosphorylation after RYGB rapidly improves obesity-induced endothelial dysfunction. Pharmacological JNK inhibition mimics the endothelial protective effects of RYGB. These findings highlight the therapeutic potential of novel strategies targeting vascular JNK2 against the severe cardiovascular disease associated with obesity. **(*J Am Heart Assoc*. 2017;6:e006441. DOI: 10.1161/JAHA.117.006441.)**

Key Words: bariatric surgery • c-Jun N-terminal kinase • endothelial function • glucagon-like peptide-1 • NO • obesity

Obesity is associated with comorbidities, such as type 2 diabetes mellitus and dyslipidemia, which increase cardiovascular risk and mortality.[1,2] In obesity, a systemic chronic inflammation leads to oxidative stress, insulin resistance, and endothelial dysfunction.[3,4] Bariatric surgery, in particular Roux-en-Y gastric bypass (RYGB), is the most effective treatment against obesity.[1] RYGB achieves sustained weight loss and significant long-term improvement of comorbidities; it also reduces cardiovascular morbidity and mortality.[1,5,6] In addition to weight loss, surgery-specific changes of

Center for Molecular Cardiology, University of Zurich, Switzerland; University Heart Center, Cardiology, University Hospital Zurich, Switzerland (P.D., V.M., M.E., S.S., G.G.C., C.M.M., T.F.L., E.O.); Institute of Clinical Chemistry, University Hospital Zurich, Zurich, Switzerland (L.R.); Institute of Veterinary Physiology (P.D., E.T.) and Laboratory for Animal Model Pathology, Institute for Veterinary Pathology (G.P.), Vetsuisse Faculty University of Zurich, Switzerland; Zurich Center for Integrative Human Physiology, University of Zurich, Switzerland (P.D., E.T., S.S., L.R., G.G.C., C.M.M., T.A.L., T.F.L., E.O.); Department of Surgery, Cantonal Hospital Fribourg, Fribourg, Switzerland (T.B.); Laboratory of Cardiovascular Endocrinology, Istituto di Ricovero e Cura a Carattere Scientifico San Raffaele Pisana, Rome, Italy (V.M.); Department of Cardiac, Thoracic and Vascular Sciences, University of Padova, Italy (F.T.); State Key Laboratory for Pharmaceutical Biotechnologies & Department of Pharmacology & Pharmacy, Li Ka Shing Faculty of Medicine, The University of Hong Kong; (P.M.V.); and Laboratory of Translational Nutrition Biology, Federal Institute of Technology Zurich (ETHZ), Schwerzenbach, Switzerland (E.O.).

Accompanying Data S1 and Figures S1 through S7 are available at http://jaha.ahajournals.org/content/6/11/e006441/DC1/embed/inline-supplementary-material-1.pdf

Correspondence to: Elena Osto, MD, PhD, Laboratory of Translational Nutrition Biology, Federal Institute of Technology Zurich (ETHZ), Schorenstrasse 16, 8603 Schwerzenbach, and Center for Molecular Cardiology, University of Zurich, Wagistrasse 12, 8952 Schlieren, Switzerland. E-mails: elena.osto@hest.ethz.ch; elena.osto@uzh.ch

Received May 1, 2017; accepted October 13, 2017.

Clinical Perspective

What Is New?

- In a rodent model of diet-induced obesity, c-Jun N-terminal kinase 2 (JNK2), but not JNK1, phosphorylation was specifically increased in the aorta.
- Roux-en-Y gastric bypass surgery restored obesity-induced vascular dysfunction by blunting JNK2-vascular activation.
- Aortic inhibition of the JNK isoform 2 after Roux-en-Y gastric bypass was associated with improved insulin and glucagon-like peptide-1–mediated endothelium-dependent vasorelaxation as a result of preserved NO bioavailability and blunted oxidative stress.
- In vivo treatment with 2 different JNK inhibitors improved endothelium-mediated vasodilation and decreased aortic JNK2 phosphorylation, thus mimicking the effect of Roux-en-Y gastric bypass.

What Are the Clinical Implications?

- Our data suggest that novel drugs that selectively blunt JNK2 activation without the downsides of available JNK inhibitors may become a promising therapeutic option against obesity-induced endothelial dysfunction and its associated cardiovascular disease.
- It will be important to assess the vascular and metabolic effects of a combination therapy of Roux-en-Y gastric bypass and JNK inhibition.
- It is intriguing to hypothesize that, as a result of such dual treatment, a higher increase in circulating glucagon-like peptide-1 and/or in other gut hormones may synergistically potentiate the benefits observed in the present experiments.

gut hormones, like glucagon-like peptide-1 (GLP-1) and bile acids, may contribute to these improvements.[7–9]

The c-Jun N-terminal kinase (JNK) family of proteins links obesity with insulin resistance and endothelial dysfunction. Of the 3 known JNK isoforms, JNK1 and JNK2 are expressed ubiquitously, whereas JNK3 expression is restricted to the brain, heart, and testes.[10] On activation, JNK suppresses cellular insulin signaling via inhibitory phosphorylation of insulin receptor substrate-1 (IRS-1) at Ser307 (Ser307–IRS-1).[11] In obese mice, whole-body deletion of JNK1 (*JNK1*$^{-/-}$), but not of JNK 2 (*JNK2*$^{-/-}$), decreased total JNK activity in liver, muscle, and adipose tissue, and reduced hepatic Ser307–IRS-1 phosphorylation.[12] This blunted weight gain and improved glucose tolerance and insulin sensitivity.[12] The deletion of JNK2, performed either globally or specifically in the liver, was also associated with the same favorable metabolic profile[13,14] previously attributed to JNK1 deletion. Hence, the in vivo tissue-specific interactions between the 2 JNK isoforms deserve further investigation under physiological and pathological conditions.[12–14]

JNK is also critical in the pathophysiology of cardiovascular disease. *JNK2*$^{-/-}$ mice are protected from hypercholesterolemia-induced oxidative stress, endothelial dysfunction,[15] and atherosclerosis.[16] JNK2 may inhibit endothelial NO synthase (eNOS) by phosphorylation at Ser116 (Ser116-eNOS).[17,18] Total JNK activation and Ser307–IRS-1 phosphorylation, which are increased in the aorta of spontaneously hypertensive rats, are associated with vascular insulin resistance.[19] Furthermore, in rat aortic rings, the JNK inhibitor SP600125[20] promotes vasodilation.[21] However, SP600125 is not JNK specific and targets other kinases.[22,23] This drawback prompted the development of more JNK-specific inhibitors (eg, the peptide inhibitor D-JNKi-1 [D-JNK]), which more selectively blocks all JNK isoforms.[24] Two-week treatment of obese diabetic *db/db* mice with the L-enantiomer of D-JNK improves glucose tolerance and insulin sensitivity, increases protein kinase B (Akt) activation, and decreases Ser307–IRS-1 phosphorylation in liver, fat, and muscle.[25] Moreover, D-JNK treatment exerts neuroprotective effects in mouse models of cerebral ischemia, and the compound is in preclinical trials.[26]

RYGB decreased total JNK activation and Ser307–IRS-1 inhibitory phosphorylation in the liver of type 2 diabetic rats 2 weeks after surgery.[27] We previously showed, in obese rats, a rapid improvement of endothelial function after RYGB.[8] In the aorta, RYGB decreased total JNK phosphorylation and oxidative stress and activated the Akt/eNOS signaling pathway, improving NO bioavailability, independent of body weight loss.[8] Therefore, the present study tested if pharmacological JNK inhibition in vivo in obese rats mimics the protective endothelial effects of RYGB. Moreover, the specific contribution of vascular JNK1 versus JNK2 in obesity-induced endothelial dysfunction and in its improvement after RYGB was investigated.

Methods

An expanded description of the methods is available in Data S1.

The data, analytic methods, and study materials will be made available on request of other researchers for purposes of reproducing the results or replicating the procedure.

Antibodies and Reagents

The following commercially available antibodies were used: JNK1/2 (R&D Systems, Minneapolis, MN); phosphorylated JNK1/2 (Thr183/Tyr185) (Santa Cruz Biotechnology, Dallas, TX); IRS-1 and phosphorylated IRS-1 (Ser307), Akt and phosphorylated Akt (Ser473), protein kinase A (PKA) and phosphorylated PKA (Thr197), cAMP response element binding protein and phosphorylated cAMP response element

binding protein (Ser133), protein kinase C (PKC) α/β and phosphorylated PKCα/βII (Thr638/641), phosphorylated PKCβII (Ser660), PKCδ and phosphorylated PKCδ (Thr505), p38 mitogen-activated protein kinase (MAPK) and phosphorylated p38 MAPK (Thr180/Tyr182), p44/42 MAPK (extracellular signal regulated kinase 1/2) and phosphorylated p44/42 MAPK (extracellular signal regulated kinase 1/2) (Thr202/Tyr204) (all from Cell Signaling, Danvers MA); PKCβII (Thermo Fisher Scientific, Waltham, MA, United States); eNOS/NOS type III and phosphorylated eNOS (Ser1177) (BD Biosciences, San Jose, CA); phosphorylated eNOS Ser116 and GAPDH (both from Merck Millipore, Darmstadt, Germany); and GLP-1 receptor (Abcam, Cambridge, UK).

Other items were purchased from supplies, as indicated: high-fat high-cholesterol diet (Research Diets, New Brunswick, NJ); SP600125 (Selleckchem, Houston, TX); selective JNK inhibitor D-JNK (H-dqsrpvqpflnlttprkprpprrrqrrkkrG-NH2) and control peptide D-TAT (H-pprrrqrrkkrG-NH2) (both from Pepscan, Lelystad, The Netherlands); dimethyl sulfoxide, norepinephrine, Nω-nitro-L-arginine methyl ester, polyethylene glycol–superoxide dismutase, sodium nitroprusside, dihydroethidium, and Hoechst 33258 (all from Sigma-Aldrich, St Louis, MO); insulin (Humalog; Lilly, Indianapolis, IN); GLP-1 (7-36) amide (Bachem, Bubendorf, Switzerland); nicotinamide ADP/reduced nicotinamide ADP (NADPH) assay kit (Abcam); cyclic GMP ELISA kit (Cell Biolabs, San Diego, CA); active GLP-1 kit (Meso Scale Discovery, Gaithersburg, MD); Microvette with or without EDTA vacutainers (Sarstedt, Nümbrecht, Germany); DPPIV inhibitor (Millipore, Darmstadt, Germany); positive-charged slides, Superfrost Plus (Thermo Scientific, Waltham, MA); RNeasy Mini Kit (Qiagen, Hilden, Germany); Ready-To-Go You-Prime First-Strand Beads (GE Healthcare, Little Chalfont, UK); and specific primers for quantitative polymerase chain reaction (Microsynth, Balgach, Switzerland).

Animals and Experimental Procedures

Male Wistar rats were fed chow (lean non–operated on age-matched controls, n=6) or a high-fat high-cholesterol diet to induce obesity (60% kcal fat and 1.25% cholesterol; n=46) for 7 weeks before and after surgery.[8] Obese rats were randomized to RYGB or sham surgery, and all procedures were performed as described.[8] Treatments started on the day after surgery. A pilot (proof-of-concept) study and a main experiment were performed with the 2 JNK inhibitors most commonly used for in vivo investigations.[20,24] In the pilot study, sham–operated rats received SP600125, 40 mg/kg per day SC (SP600125, n=8), or vehicle dimethyl sulfoxide sc ($control_{DMSO}$, n=6). The main experiment compared RYGB (n=10) with sham–operated ad libitum–fed rats treated for 8 days with either the selective JNK inhibitor D-JNK (once-daily sc injection of 20 mg/kg per day; H-dqsrpvqpflnlttprkprpprrrqrrkkrG-NH2; n=13) or an equimolar dose (8.3 mg/kg) of the control peptide D-TAT sc ($control_{D\text{-}TAT}$; H-pprrrqrrkkrG-NH2; n=9). Some $control_{D\text{-}TAT}$ and D-JNK rats were kept in metabolic cages to measure water intake and urine excretion. The Cantonal Veterinary Office of Zurich (Zurich, Switzerland) approved all animal experiments (approval No. 060/2015_860).

Organ Chamber Experiments

The thoracic aorta was cut into 2- to 3-mm-long rings and connected to an isometric force transducer (Multi-Myograph 610M; Danish Myo Technology A/S, Aarhus, Denmark), suspended in an organ chamber filled with 6 mL Krebs-Ringer bicarbonate solution (37°C, pH 7.4, 95% O_2, 5% CO_2). Isometric tension was recorded continuously, as previously described.[8,15] After a 30-minute equilibration period, rings were gradually stretched to reach the optimal point of their length-tension curve, as determined by the contraction in response to potassium chloride (100 mmol/L). During submaximal contraction to norepinephrine (3×10^{-6} mol/L), concentration-relaxation curves were obtained in a cumulative manner in response to insulin (10^{-11} to 10^{-5} mol/L) and GLP-1 (7-36) amide (10^{-12} to 10^{-6} mol/L).[28,29] Responses to insulin and GLP-1 were recorded in the presence or absence of Nω-nitro-L-arginine methyl ester (10^{-4} mol/L), a nonselective NO synthase inhibitor, or of the free radical scavenger polyethylene glycol–superoxide dismutase (150 U/mL). To study the direct vascular effects of D-JNK, a subset of aortic rings were incubated ex vivo for 30 minutes with 5 μmol/L D-JNK before insulin or GLP-1. The NO donor sodium nitroprusside (10^{-10} to 10^{-5} mol/L) was added to test endothelium-independent vasodilation. Relaxations were expressed as a percentage of the precontraction with norepinephrine.

Western Blot Analysis

Frozen aortas were pulverized and dissolved in lysis buffer: NaCl (120 mmol/L), Tris (50 mmol/L), NaF (20 mmol/L), benzamidine (1 mmol/L), dithiothreitol (1 mmol/L), EDTA (1 mmol/L), EGTA (6 mmol/L), sodium pyrophosphate (15 mmol/L), p-nitrophenyl phosphate (30 mmol/L), phenylmethylsulfonyl fluoride (0.1 mmol/L), leupeptin (0.8 μg/mL), and NP-40 (1%). Analysis was performed with antibodies listed in the Antibodies and Reagents subsection.

In Vitro Assays

NADPH oxidase activity, cGMP levels, and fasting plasma concentrations of active GLP-1 were measured using commercial kits listed in the Antibodies and Reagents subsection.

Statistical Analysis

Quantitative data are presented as mean±SD or median with interquartile range. Statistical analysis was conducted with unpaired Student *t* test or by 1-way ANOVA, followed by the Bonferroni post hoc test, as appropriate. Two-way ANOVA with repeated measures was used to compare repeated measurements in the same animals. Data were subjected to the statistical analysis after a test of the data distribution status using the Kolmogorov-Smirnov test. If the homogeneity of variance assumption was violated, the nonparametric Kruskal-Wallis test was used instead.

All tests were 2 sided, and statistical significance was accepted if the null hypothesis could be rejected at $P<0.05$. All analyses were performed with GraphPad Prism Software (version 7).

Results

In Vivo Pharmacological JNK Inhibition Improves Obesity-Induced Endothelial Dysfunction Similar to RYGB

Aortic relaxation in response to GLP-1 and insulin improved similarly after D-JNK and RYGB when compared with obese control$_{D\text{-}TAT}$ animals (Figure 1A and 1B). Vasodilation was abolished by preincubation with the eNOS inhibitor Nω-nitro-L-arginine methyl ester, indicating an endothelial NO-dependent mechanism (Figure S1A and S1B). Beforehand, we showed that in lean non–operated age-matched and chow-fed male Wistar rats, D-JNK did not alter GLP-1's and insulin's baseline vasodilatory effects compared with vehicle-treated controls (Figure S1C and S1D). Results after D-JNK treatment strengthened the findings of the pilot experiment (Figure S1E and S1F), in which rats receiving the JNK inhibitor SP600125 also improved vascular relaxation, although the effect was less pronounced than after RYGB.

Vascular JNK Inhibition Improves Endothelial Function in Control$_{D\text{-}TAT}$ Rats

To test whether the improved relaxation seen in D-JNK rats resulted from the direct vascular benefits of JNK inhibition, a subset of aortic rings isolated from D-JNK and control$_{D\text{-}TAT}$ rats were preincubated with 5 μmol/L D-JNK for 30 minutes ex vivo[21,24] before organ chamber experiments. Insulin- and GLP-1–induced relaxations improved in control$_{D\text{-}TAT}$ rings treated ex vivo with D-JNK compared with untreated rings, suggesting a direct aortic action of D-JNK (Figure 1C and 1D). By contrast, ex vivo D-JNK preincubation did not further ameliorate the response of aortas from the rats that had received D-JNK for 8 days (Figure 1E and 1F).

In Vivo JNK Inhibition and RYGB Reduce Aortic JNK2 Phosphorylation Induced by Obesity

Next, we assessed the specific contribution of the 2 vascular JNK isoforms in obesity-induced endothelial dysfunction. Phosphorylation of JNK2, but not of JNK1, increased in aortas of obese control$_{D\text{-}TAT}$ when compared with chow-fed lean D-TAT rats (Figure 2A). Furthermore, aortic JNK2 phosphorylation was significantly decreased in RYGB and D-JNK–treated rats compared with obese control$_{D\text{-}TAT}$ rats, whereas JNK1 phosphorylation was not affected (Figure 2B). A similar result was obtained after the pilot treatment with SP600125 (Figure S2A).

JNK Inhibition Restores Vascular Insulin- and GLP-1–Dependent Akt/eNOS/NO Pathway Similar to RYGB

The vascular Akt/eNOS signaling, which is activated by insulin and GLP-1[8,28] and inhibited by JNK,[11,17] was assessed by Western blotting in aortic lysates. The JNK-dependent inhibitory Ser307–IRS-1 phosphorylation decreased comparably after RYGB and D-JNK (Figure 2C), whereas the activatory Akt-Ser473 phosphorylation increased (Figure 2D). This led to enhanced phosphorylation of the activatory eNOS-Ser1177 (Figure 3A), a favorable dimer/monomer ratio of eNOS (Figure 3B), which is essential for the proper coupling and function of the enzyme.[30,31] Finally, it augments NO production, as assessed by increased aortic cGMP levels (Figure 3C). In vivo SP600125 treatment also protected the insulin- and GLP-1–dependent vascular signaling pathway, leading to preserved NO bioavailability (Figure S2B through S2E). The phosphorylation of Ser116 is a putative JNK2 target for the inhibition of eNOS.[17,18] However, its assessment was inconclusive because of lack of specificity of the commercially available anti–phosphorylated Ser116-eNOS antibody in rat aortic tissue (Figure S3). Additional players able to modulate vascular insulin resistance,[32–34] such as PKC (α/β, β II, and δ; Figure S4A through S4C) and extracellular signal regulated kinase 1/2 (p44 and p42; Figure S4E), were assessed. No difference in phosphorylation was observed between controls and rats after RYGB or JNK inhibition, which further supports the role of reduced aortic JNK2 phosphorylation as a crucial mediator of the vascular benefits of RYGB. Only the phosphorylation of p38 MAPK was increased on JNK inhibition and unchanged in control and RYGB rats (Figure S4D), which may be a potential off-target effect of long-term systemic in vivo D-JNK treatment.

JNK Inhibition Reduces Vascular Oxidative Stress Similar to RYGB

JNK enhances vascular oxidative stress, which, in turn, reduces NO bioavailability and leads to endothelial

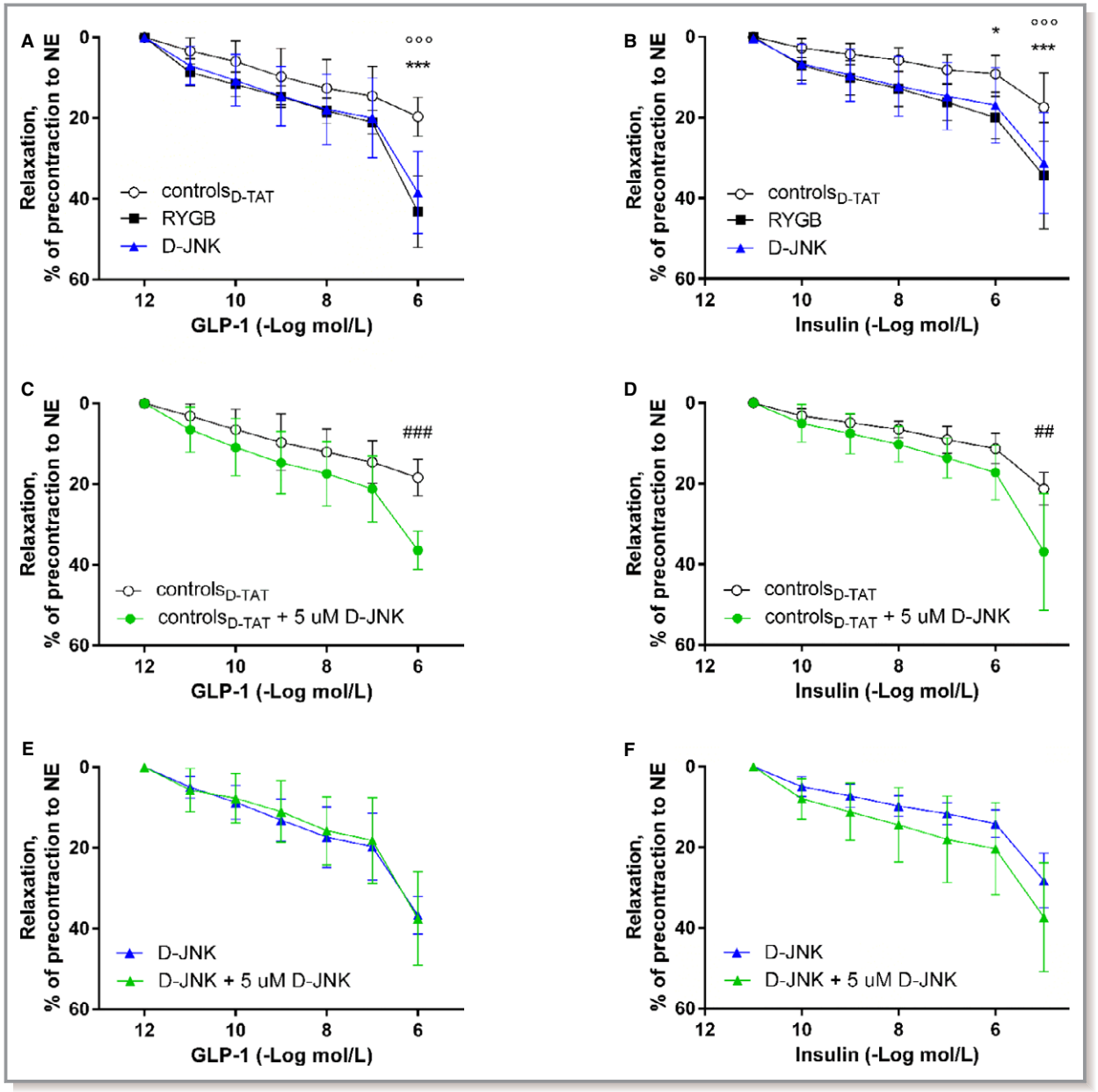

Figure 1. Cumulative concentration-response curves of aortic rings isolated 8 days after Roux-en-Y gastric bypass (RYGB) or sham surgery/start of treatment after submaximal contraction to norepinephrine in response to glucagon-like peptide-1 (GLP-1; A) and insulin (B) in RYGB rats, control$_{D\text{-}TAT}$ rats, and rats treated with the peptide inhibitor D-JNKi-1 (D-JNK rats) (n=7–13 per group). Ex vivo relaxation of aortic rings with or without 30 minutes ex vivo preincubation with 5 µmol/L D-JNK. Concentration-response curves after submaximal contraction to norepinephrine in response to GLP-1 (C) and insulin (D) in control$_{D\text{-}TAT}$ rats and to GLP-1 (E) and insulin (F) in D-JNK rats (n=3–6 per group). Results are evaluated by 2-way repeated measures ANOVA and Bonferroni post hoc test. Data are shown as mean±SD. $^{*}P<0.05$, $^{***}P<0.001$ for RYGB vs control$_{D\text{-}TAT}$; $^{°°°}P<0.001$ for control$_{D\text{-}TAT}$ vs D-JNK; $^{\#\#}P<0.01$, $^{\#\#\#}P<0.001$ for control$_{D\text{-}TAT}$ vs D-TAT preincubated 30 minutes ex vivo with 5 µmol/L D-JNK.

dysfunction.[35,36] Decreased oxidative stress after RYGB protects endothelial function.[8] Therefore, it was further assessed if in vivo JNK inhibition also mimics the effect of RYGB on the vascular reduction-oxidation balance. Preincubation with the free radical scavenger superoxide dismutase improved relaxation in response to insulin and GLP-1 only in aortic rings of control$_{D\text{-}TAT}$ rats. No further improvements were observed in RYGB- and D-JNK–treated rats, which suggests markedly reduced oxidative stress in these contexts (Figure 3D and 3E). Concurrent with this notion, dihydroethidium staining of aortic sections showed decreased superoxide anion (O_2^-) levels after RYGB and after D-JNK treatment (Figure 3F). NADPH oxidase activity, which contributes to the generation of O_2^-,[35] was also significantly decreased in the

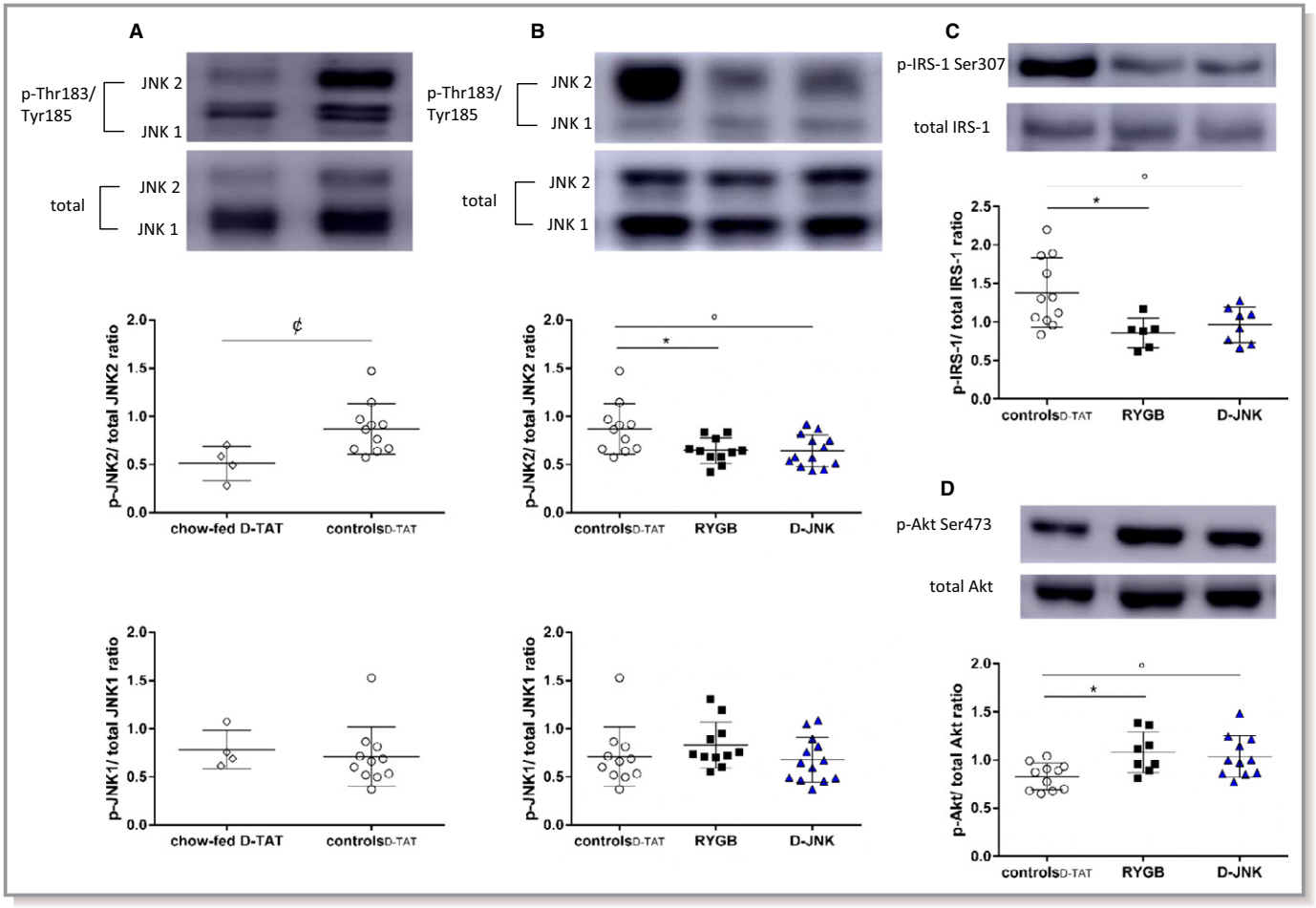

Figure 2. (A), c-Jun N-terminal kinase (JNK) 1 and JNK2 phosphorylation (46 and 55 kDa, respectively) in the aortas of lean chow-fed D-TAT vs obese control$_{D\text{-}TAT}$ rats (determined by unpaired *t* test). Phosphorylation of aortic JNK1 and JNK2 (B), insulin receptor substrate-1 (IRS-1) Ser307 (C), and protein kinase B (Akt) Ser473 (D) in control$_{D\text{-}TAT}$, Roux-en-Y gastric bypass (RYGB), and peptide inhibitor D-JNKi-1 (D-JNK) rats 8 days after surgery/start of treatment. Representative Western blots and densitometric quantifications are shown (determined by 1-way ANOVA and Bonferroni post hoc test; n=4–13 per group). Results are shown as mean±SD. p indicates phosphorylated. $^{¢}P<0.05$ for chow-fed control peptide D-TAT vs control$_{D\text{-}TAT}$, $^{*}P<0.05$ for RYGB vs control$_{D\text{-}TAT}$, $^{°}P<0.05$ for control$_{D\text{-}TAT}$ vs D-JNK.

aortas of both RYGB and D-JNK rats, thus contributing to preserved NO bioavailability (Figure 4A). Similar results were obtained after SP600125 treatment (Figure S5A and S5B).

GLP-1 Contributes to Vascular JNK2 Inhibition After RYGB

Increased circulating GLP-1 contributes to the beneficial cardiovascular effects of RYGB.[8,9] GLP-1–dependent PKA activation inhibits JNK1 and JNK2 in various tissues, including the endothelium,[34,37] where it also activates the Akt/eNOS pathway.[38,39] In line with our previous results,[8] fasting plasma GLP-1 levels were increased after RYGB (Figure 4B). Surprisingly, D-JNK treatment also increased GLP-1 levels compared with control$_{D\text{-}TAT}$ rats, although to a lesser extent than RYGB (Figure 4B). By contrast, SP600125 did not affect circulating GLP-1 levels (Figure S5C). The aortic expression of the GLP-1 receptor was up-regulated in RYGB and D-JNK rats. This was accompanied downstream by enhanced phosphorylation of the PKA isoform C-α at Thr197 and of the cAMP response element binding protein at Ser133 (Figure 4C through 4E), which lie upstream of JNK1 and JNK2 inhibition.[34,37] To further ascertain the role of GLP-1 in modulating JNK2 phosphorylation after RYGB, we analyzed aortas from our previous study, in which sham–operated on rats were treated with the GLP-1 analogue liraglutide and RYGB rats received the GLP-1 receptor antagonist exendin-9 for 8 days after surgery.[8] JNK2 phosphorylation remained high in RYGB rats on GLP-1 receptor blockade, whereas liraglutide treatment in sham–operated on rats decreased JNK2 phosphorylation. JNK1 phosphorylation was unchanged in all groups (Figure 5A). These results suggest that vascular JNK2 inactivation may contribute to the GLP-1–dependent improvement of endothelial

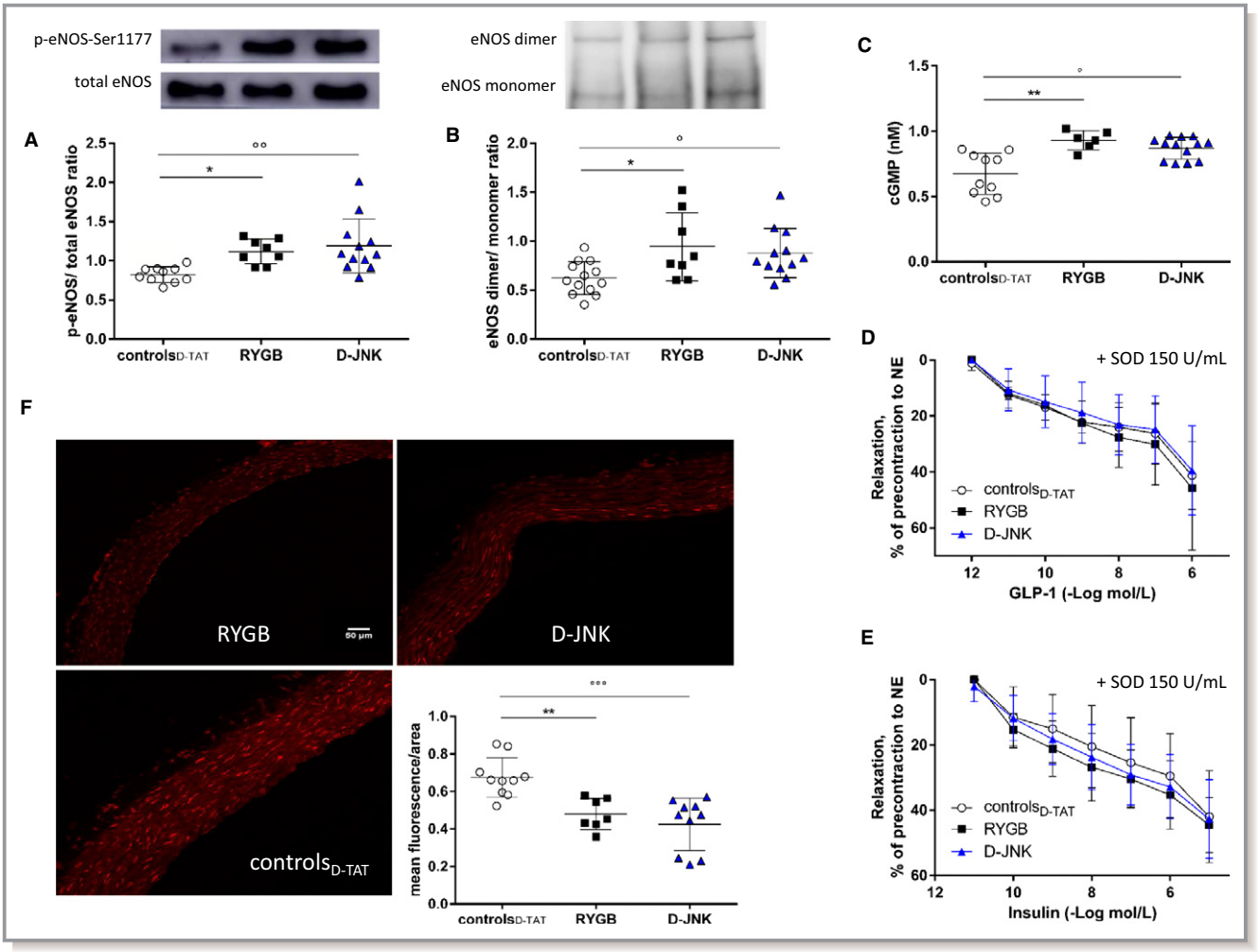

Figure 3. (A) Endothelial NO synthase (eNOS) Ser1177 phosphorylation (p-eNOS); and eNOS dimerization (B). Representative Western blots and densitometric quantifications are shown (determined by 1-way ANOVA and Bonferroni post hoc test; n=6–13 per group). (C), In vitro quantification of cGMP levels in $control_{D\text{-}TAT}$, Roux-en-Y gastric bypass (RYGB), and peptide inhibitor D-JNKi-1 (D-JNK) rats 8 days after surgery/start of treatment (determined by Kruskal-Wallis test and Dunn multiple comparison test; n=6–13 per group). Effect of preincubation with 150 U/mL of polyethylene glycol–superoxide dismutase (SOD) on the endothelium-dependent relaxation to glucagon-like peptide-1 (GLP-1); (D) and insulin (E) in the same experimental groups (no differences, determined by 2-way repeated measures ANOVA and Bonferroni post hoc test; n=3–9 per group). F, Representative pictures of dihydroethidium fluorescent staining of superoxide anions and relative quantification in aortas isolated 8 days after surgery from $control_{D\text{-}TAT}$, RYGB, and D-JNK rats (determined by 1-way ANOVA and Bonferroni post hoc test; n=7–10 per group). Results are shown as mean±SD (A, B, and F) or median±interquartile range (C). *P<0.05, **P<0.01 for RYGB vs $control_{D\text{-}TAT}$; °P<0.05, °°P<0.01, °°°P<0.001 for $control_{D\text{-}TAT}$ vs D-JNK.

dysfunction seen after RYGB.[8] In line with previous results,[8] RYGB reduced food intake and body weight (Figure 5B and 5C). D-JNK treatment affected food intake and body weight similar to RYGB (Figure 5B and 5C), whereas SP600125 had no effect on these 2 parameters compared with its vehicle (Figure S6A and S6B). Non–operated chow-fed rats treated for 8 days with D-TAT and D-JNK did not show differences in body weight between the 2 groups (Figure S6C). This difference between the 2 JNK inhibitors prompted additional investigations to assess potential toxicity associated with the pharmacological treatment (Figure S7), as described in Data S1.

Discussion

JNKs link metabolic to cardiovascular disease.[8,12,14,15,17,18] The novel findings of this study show that RYGB via GLP-1–dependent signaling improves obesity-induced endothelial dysfunction by specific inhibition of aortic JNK2 phosphorylation. We provide the following key observations: (1) obesity specifically increased JNK2, but not JNK1, phosphorylation in the aorta; (2) RYGB improved endothelial function via a specific decrease of aortic JNK2 phosphorylation; (3) in vivo pharmacological JNK inhibition rapidly mimics this beneficial vascular effect; and (4) on lower JNK2 phosphorylation, the

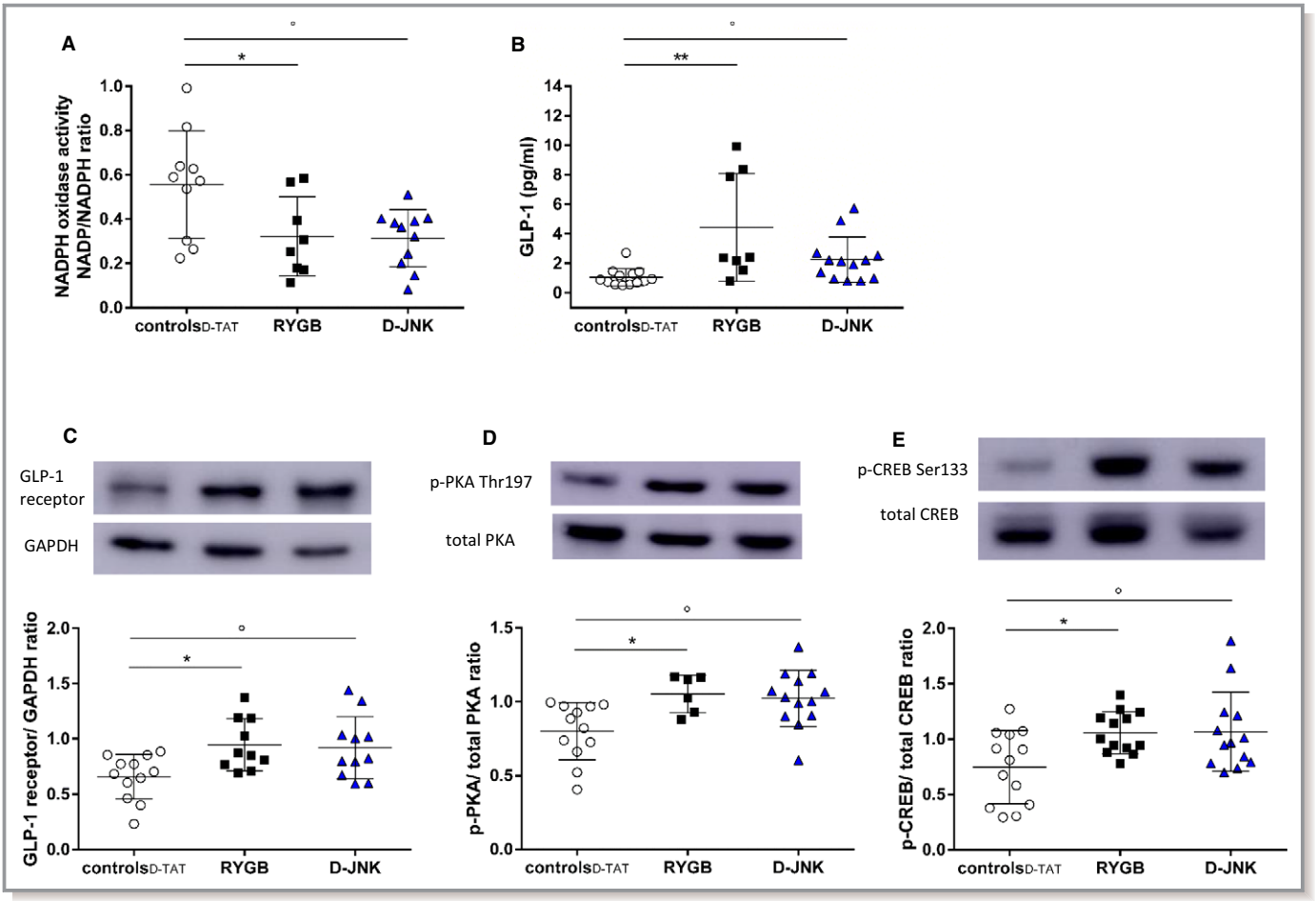

Figure 4. (A), Reduced nicotinamide ADP (NADPH) oxidase activity in aortas (determined by 1-way ANOVA and Bonferroni post hoc test; n=6–13 per group). (B), Fasting plasma glucagon-like peptide-1 (GLP-1) levels in control$_{D\text{-}TAT}$, Roux-en-Y gastric bypass (RYGB), and peptide inhibitor D-JNKi-1 (D-JNK) rats 8 days after surgery/start of treatment (determined by Kruskal-Wallis test and Dunn multiple comparison test; n=6–13 per group). Aortic GLP-1 receptor expression (C) and phosphorylation of protein kinase A (p-PKA) C-α Thr197 (D) and cAMP response element binding protein (p-CREB) Ser133 (E) in the same groups. Representative Western blots and densitometric quantifications are shown (determined by 1-way ANOVA and Bonferroni post hoc test; n=6–13 per group). Results are shown as mean±SD (A and C-E) or median±interquartile range (B). **P*<0.05, ***P*<0.01 for RYGB vs all other groups; °*P*<0.05 for control$_{D\text{-}TAT}$ vs D-JNK.

insulin- and GLP-1–dependent Akt/eNOS signaling was restored, oxidative stress was decreased, and aortic NO bioavailability was preserved. The major results and proposed underlying mechanisms are summarized in Figure 6.

RYGB Reduces Aortic JNK2 Phosphorylation Induced by Obesity and Protects Endothelial Function

Studies using tissue-specific gene targeting in mice pointed initially to JNK1[12,14] and later to JNK2[13] as pivotal players in the pathophysiological characteristics of obesity and type 2 diabetes mellitus. Hence, the role of the 2 isoforms in the overall JNK activity in metabolic disease is yet unclear. *JNK2*$^{-/-}$ mice were protected against hypercholesterolemia-induced endothelial dysfunction[15] and atheroma formation,[16] which may suggest a specific contribution of JNK isoform 2 in the pathophysiological characteristics of atherosclerotic disease. We and others described also the association between total JNK activation and endothelial dysfunction induced by obesity[8,40] and type 2 diabetes mellitus[41]; however, the role of JNK1 versus JNK2 has not yet been elucidated in this context.

Our study shows that in obesity, enhanced aortic-specific JNK2 phosphorylation impairs the insulin/IRS-1– and GLP-1/GLP-1 receptor–dependent Akt/eNOS/NO pathway, leading to endothelial dysfunction, whereas JNK1 phosphorylation remains unchanged. Indeed, RYGB reduces JNK2 hyperphosphorylation and, thus, preserves the common insulin- and GLP-1–mediated Akt/eNOS-dependent NO production and restores endothelial function.[29] RYGB-mediated specific JNK2 inhibition was associated with decreased aortic Ser307–IRS-1

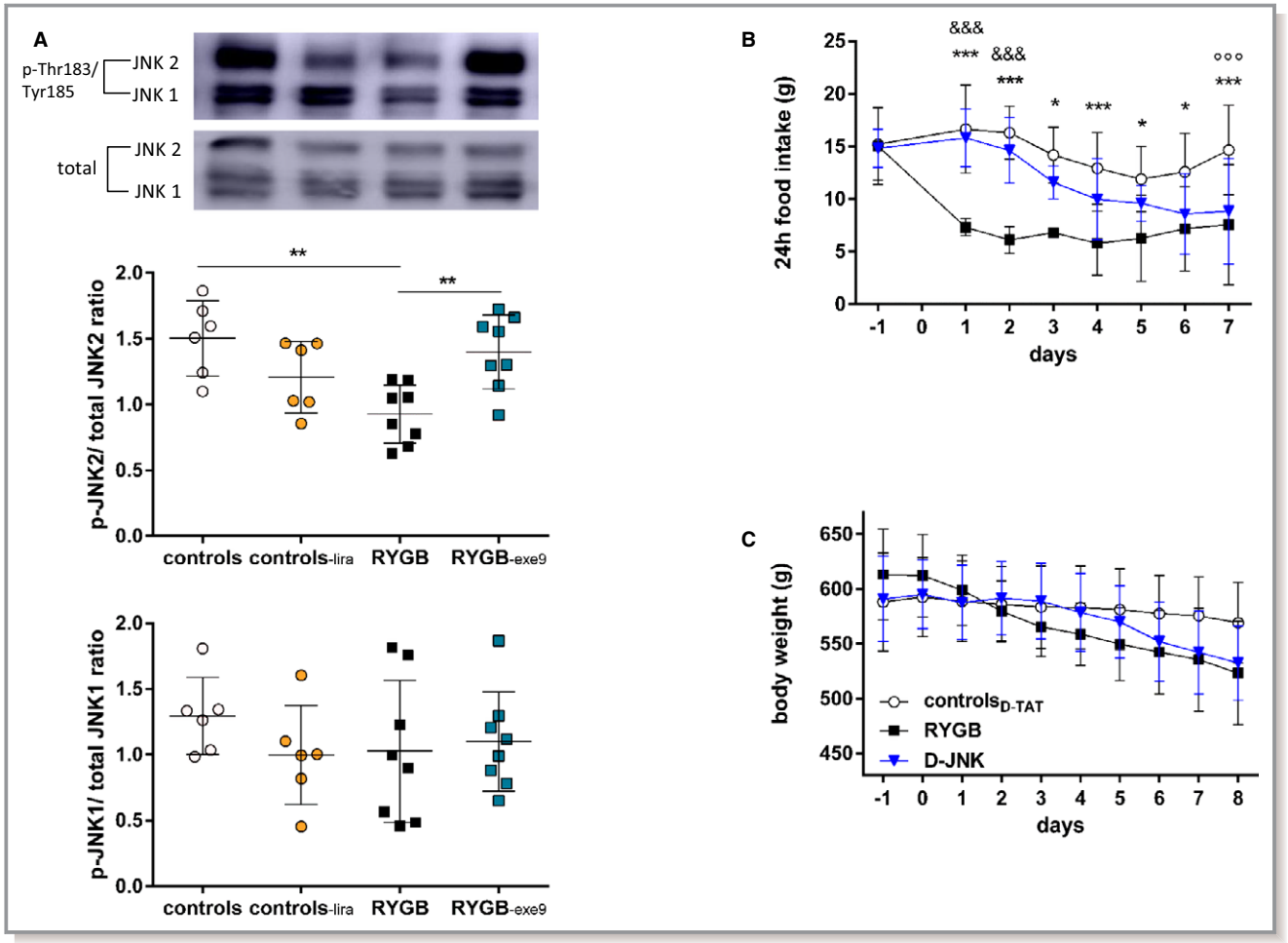

Figure 5. (A), Aortic c-Jun N-terminal kinase (JNK) 1 and JNK2 phosphorylation in sham–operated on rats treated with vehicle (controls) or liraglutide, 0.2 mg/kg BID sc (controls$_{-lira}$), and Roux-en-Y gastric bypass–operated on rats treated with vehicle (RYGB) or exendin$_{-9}$, 10 μg/kg per hour (RYGB$_{-exe9}$), for 8 days. Tissues were taken from rats of a previous study on day 8 after surgery or after the start of treatment, respectively[8] (determined by 1-way ANOVA and Bonferroni post hoc test; n=8–13 per group). Cumulative 24-hour food intake (determined by 2-way ANOVA and Bonferroni post hoc test; n=8–13 per group; (B) and body weight (C) of control$_{D-TAT}$, RYGB, and peptide inhibitor D-JNKi-1 (D-JNK) rats before and after surgery and start of treatment (day 0) (no differences, determined by 2-way repeated measures ANOVA and Bonferroni post hoc test; n=8–13 per group). Results are shown as mean±SD. p indicates phosphorylated. *P<0.05 and **P<0.01 for RYGB vs controls or RYGB$_{-exe9}$; ***P<0.001 for RYGB vs control$_{D-TAT}$; $^{\&\&\&}P$<0.001 for RYGB vs D-JNK; °°°D-JNK vs control$_{D-TAT}$.

phosphorylation. To date, the inhibitory Ser307–IRS-1 phosphorylation has been linked to total JNK activity in the context of hepatic insulin resistance.[12] Only one study in spontaneously hypertensive rats linked Ser307–IRS-1 phosphorylation to aortic insulin resistance as a result of total JNK increased activity, with no further investigations on JNK isoform specificity.[19]

In Vivo Inhibition of JNK Mimics the Endothelial Protective Effects of RYGB

In vivo treatment with 2 different JNK inhibitors improved endothelium-mediated vasodilation and decreased aortic JNK2 phosphorylation. Activation of the intracellular Akt/eNOS signaling led to higher NO production, thus mimicking the effect of RYGB. D-JNK treatment decreased weight loss and food intake equally to RYGB; however, body weight loss per se is not sufficient to improve endothelial function, as previously shown in sham–operated rats whose body weight loss was matched to RYGB by food restriction.[8] We observed that in rats that were body weight matched to RYGB rats, endothelial dysfunction persisted and was associated with increased total JNK phosphorylation at the aortic level.[8] Furthermore, the pilot study showed that the favorable impact of SP600125 on endothelial function can also be achieved in the absence of body weight loss or reduced eating, suggesting a specific vascular benefit on pharmacological JNK inhibition. In addition, short-term ex vivo D-JNK treatment improved vasodilation of aortas of control$_{D-TAT}$ rats but had no incremental benefit in animals receiving long-term in vivo D-JNK treatment. These

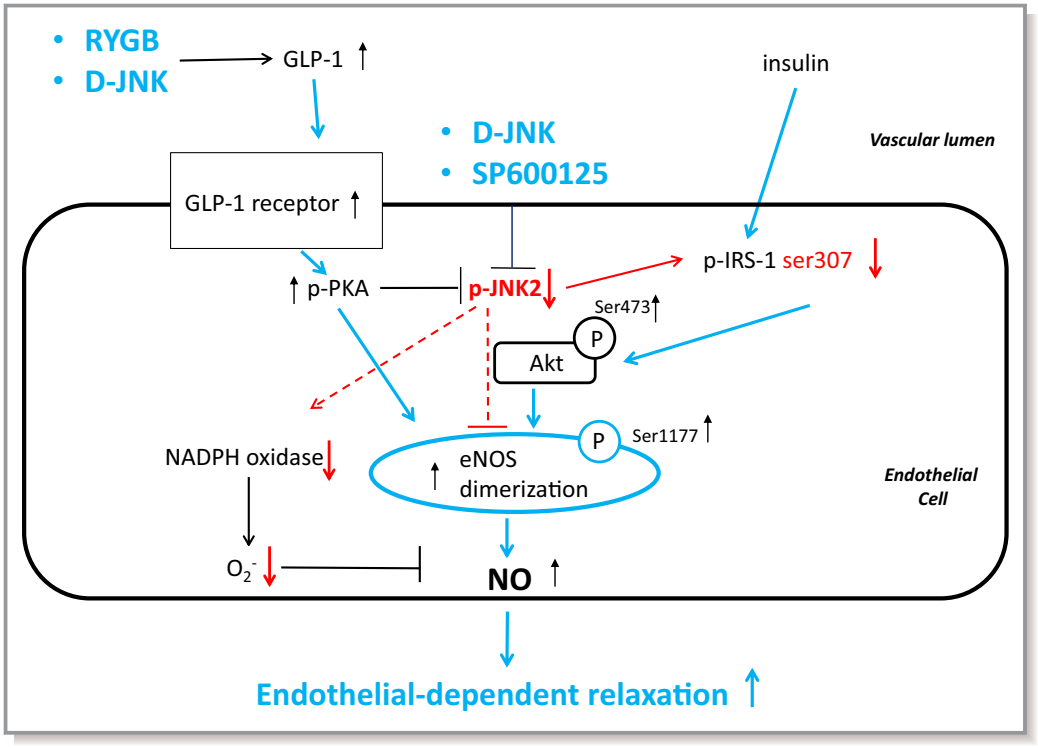

Figure 6. Proposed mechanism(s) underlying the improvement of endothelium-dependent vasodilation after Roux-en-Y gastric bypass (RYGB). Higher circulating glucagon-like peptide-1 (GLP-1) after RYGB activates the endothelial GLP-1 receptor and downstream protein kinase A (PKA), which inhibits c-Jun N-terminal kinase (JNK) 2. JNK2 directly inhibits endothelial NO synthase (eNOS) and insulin receptor substrate-1 (IRS-1) in the insulin signaling pathway; PKA and IRS-1 lead to protein kinase B (Akt) activation, which then directly stimulates eNOS. This, in turn, leads to improved NO bioavailability and vasodilation. In parallel, JNK2 inactivation inhibits reduced nicotinamide ADP (NADPH) oxidase activity and decreases the levels of superoxide anions, which further contributes to preserved NO bioavailability and vasodilation. These beneficial effects of RYGB were mimicked by in vivo pharmacological JNK inhibition. Blue and red arrows indicate experimentally observed activation and inactivation, respectively, of proposed downstream mediators. D-JNK indicates peptide inhibitor D-JNKi-1; and p, phosphorylated.

findings support a JNK inhibitory effect directly exerted in the aortas to complement other systemic beneficial metabolic effects of in vivo D-JNK treatment.[25,42]

JNKs promote reactive oxygen species production, which impairs NO bioavailability and leads to endothelial dysfunction.[15,36] In agreement with our previous findings,[8] the preincubation of aortic rings with the radical scavenger superoxide dismutase improved insulin- and GLP-1–mediated relaxations of aortas in control$_{D\text{-}TAT}$ rats but not in RYGB and D-JNK treated rats. This result confirms the reduction of vascular oxidative stress, as shown by the reduced O_2^- levels and NADPH oxidase activity,[35] in the aortas of RYGB and D-JNK rats. In microvascular endothelial cells, NADPH-dependent increase of reactive oxygen species after hypoxia/reoxygenation was blunted by SP600125 and by dominant-negative JNK1, whereas the role of JNK2 in that condition had not been investigated in detail.[43] Our findings suggest that in the aorta, obesity may specifically induce NADPH oxidase via JNK2, rather than JNK1, activation.

GLP-1–Dependent Inhibition of Aortic JNK2 Restores Endothelial Function After RYGB

Finally, the present study focused on the role of upstream GLP-1–dependent molecular pathways in mediating aortic JNK2 inactivation after RYGB. In line with our previous results,[8] fasting plasma GLP-1 levels and aortic GLP-1 receptor expression were increased after RYGB. GLP-1–dependent aortic PKA Thr197 and cAMP response element binding protein Ser133 activatory phosphorylations were increased and accompanied by downstream JNK2 inhibition, thus strengthening the mechanistic link between increased GLP-1 signaling after RYGB and aortic JNK2 inhibition. This notion was supported by the fact that in vivo GLP-1 receptor antagonism with exendin-9 in RYGB rats blocked the JNK2 inhibition achieved by RYGB, whereas GLP-1 agonism with liraglutide tended to mimic the benefit of RYGB in obese sham–operated on rats.

Interestingly, systemic administration of D-JNK also increased circulating GLP-1 levels; this was not observed with SP600125, possibly because of its lower potency and specificity.[23] Peripheral GLP-1 is secreted from intestinal endocrine cells in response to nutrients[44] and insulin.[45] Therefore, JNK inhibition in the small intestine may influence GLP-1 secretion through the insulin signaling. Hence, systemic JNK inhibition may improve endothelium-mediated vasodilation through a direct inactivation of vascular JNK2, and indirectly through increased GLP-1 signaling, which may further contribute to blunt JNK2 and to activate eNOS in aortas, as summarized in Figure 6. In future studies, it would, therefore, be important to assess the vascular and metabolic effects of a combination therapy between RYGB and JNK inhibition in comparison to the single treatment reported in the present study. It is intriguing to hypothesize that, as a result of such dual treatment, higher increases in circulating GLP-1 and/or in other gut hormones may synergistically potentiate the benefits observed in the present experiments.

Study Limitations

Reduced JNK2-dependent inhibitory phosphorylated Ser116-eNOS may have contributed to the observed benefits of RYGB and JNK inhibition,[17,18] but lack of specificity of the commercially available antibodies in the rat aorta did not allow a satisfactory assessment of this putative JNK2 target.

SP600125 inhibits multiple other kinases besides JNK,[23] which limits its clinical application. On the other hand, D-JNK treatment, despite a high JNK specificity,[24] may induce renal toxicity, in particular in obese animals, which seems attributable to its carrier peptide, D-TAT, and thus is independent of the D-JNK inhibitory activity, as previously shown.[46] Indeed, we observed proximal tubule injury in the carrier peptide–treated control$_{D\text{-}TAT}$ and in D-JNK rats. In a previous study, despite improved glucose control, albuminuria worsened after in vivo treatment with the peptide JNK inhibitor in diabetic *db/db* mice[42] by an effect possibly linked to the D-TAT carrier peptide–induced kidney toxicity, independent of the metabolic benefits of JNK inhibition.[42,46] In our study, SP600125 treatment was not associated with kidney injury, further supporting the presence of JNK-independent cytotoxicity (ie, toxicity related to the D-TAT carrier peptide).[46] Last, in D-JNK treated rats, aortic phosphorylation of p38 MAPK was increased, in contrast to previous in vitro studies testing D-JNK specificity.[26,47] Although potential off-target effects of long-term systemic in vivo D-JNK administration cannot be excluded, in our setting, this treatment led to overall improved aortic Akt/eNOS signaling and NO bioavailability.

Overall, our data suggest that novel drugs, able to selectively blunt JNK2 activation without the downsides of available JNK inhibitors, may become a promising therapeutic option against obesity-induced endothelial dysfunction and its associated cardiovascular disease.

Conclusions

Obesity-induced activation of vascular JNK2 and the associated endothelial dysfunction were reversed by RYGB, through GLP-1–dependent signaling. These beneficial effects of RYGB were mimicked by in vivo pharmacological JNK inhibition, highlighting the potential therapeutic relevance of novel strategies targeting vascular JNK2 against the severe cardiovascular disease associated with obesity.

Acknowledgments

We thank Sara Gobbato for technical help and Amy Taheri for a critical revision of the article.

Author Contributions

The contributions to the article were as follows: study design: Osto and Lutz; study conduct, data collection, and analysis: Osto, Doytcheva, Bächler, Tarasco, Marzolla, Engeli, Pellegrini, Stivala, and Rohrer; writing: Osto, Lutz, Doytcheva, Marzolla, Tona, Camici, Vanhoutte, Matter, and Lüscher. All authors had full access and take full responsibility for the integrity of the data and the accuracy of the data analysis.

Sources of Funding

This work was supported, in part, by the University of Zurich Forschungskredit (FK-85701-02-01 to Osto and FK-15-051 to Doytcheva); the Swiss National Science Foundation Ambizione Grant (PZOOP3_161S0S/1 to Osto); the Swiss Card-Onco-Grant, Alfred and Annemarie von Sick Grant (Lutz and Osto); and the Swiss Heart Foundation (Lutz and Osto).

Disclosures

None.

References

1. Poirier P, Cornier MA, Mazzone T, Stiles S, Cummings S, Klein S, McCullough PA, Ren Fielding C, Franklin BA; American Heart Association Obesity Committee of the Council on Nutrition, Physical Activity, and Metabolism. Bariatric surgery and cardiovascular risk factors: a scientific statement from the American Heart Association. *Circulation*. 2011;123:1683–1701.
2. NCD Risk Factor Collaboration (NCD-RisC). Trends in adult body-mass index in 200 countries from 1975 to 2014: a pooled analysis of 1698 population-based measurement studies with 19.2 million participants. *Lancet*. 2016;387:1377–1396.
3. Mauricio MD, Aldasoro M, Ortega J, Vila JM. Endothelial dysfunction in morbid obesity. *Curr Pharm Des*. 2013;19:5718–5729.
4. Bays HE, Toth PP, Kris-Etherton PM, Abate N, Aronne LJ, Brown WV, Gonzalez-Campoy JM, Jones SR, Kumar R, La Forge R, Samuel VT. Obesity, adiposity, and

dyslipidemia: a consensus statement from the National Lipid Association. *J Clin Lipidol*. 2013;7:304–383.

5. Adams TD, Davidson LE, Litwin SE, Kolotkin RL, LaMonte MJ, Pendleton RC, Strong MB, Vinik R, Wanner NA, Hopkins PN, Gress RE, Walker JM, Cloward TV, Nuttall RT, Hammoud A, Greenwood JL, Crosby RD, McKinlay R, Simper SC, Smith SC, Hunt SC. Health benefits of gastric bypass surgery after 6 years. *JAMA*. 2012;308:1122–1131.
6. Brethauer SA, Heneghan HM, Eldar S, Gatmaitan P, Huang H, Kashyap S, Gornik HL, Kirwan JP, Schauer PR. Early effects of gastric bypass on endothelial function, inflammation, and cardiovascular risk in obese patients. *Surg Endosc*. 2011;25:2650–2659.
7. Laferrere B, Reilly D, Arias S, Swerdlow N, Gorroochurn P, Bawa B, Bose M, Teixeira J, Stevens RD, Wenner BR, Bain JR, Muehlbauer MJ, Haqq A, Lien L, Shah SH, Svetkey LP, Newgard CB. Differential metabolic impact of gastric bypass surgery versus dietary intervention in obese diabetic subjects despite identical weight loss. *Sci Transl Med*. 2011;3:80re82.
8. Osto E, Doytcheva P, Corteville C, Bueter M, Dorig C, Stivala S, Buhmann H, Colin S, Rohrer L, Hasballa R, Tailleux A, Wolfrum C, Tona F, Manz J, Vetter D, Spliethoff K, Vanhoutte PM, Landmesser U, Pattou F, Staels B, Matter CM, Lutz TA, Luscher TF. Rapid and body weight-independent improvement of endothelial and high-density lipoprotein function after Roux-en-Y gastric bypass: role of glucagon-like peptide-1. *Circulation*. 2015;131:871–881.
9. Seeley RJ, Chambers AP, Sandoval DA. The role of gut adaptation in the potent effects of multiple bariatric surgeries on obesity and diabetes. *Cell Metab*. 2015;21:369–378.
10. Hotamisligil GS. Role of endoplasmic reticulum stress and c-Jun NH2-terminal kinase pathways in inflammation and origin of obesity and diabetes. *Diabetes*. 2005;54(suppl 2):S73–S78.
11. Aguirre V, Uchida T, Yenush L, Davis R, White MF. The c-Jun NH(2)-terminal kinase promotes insulin resistance during association with insulin receptor substrate-1 and phosphorylation of Ser(307). *J Biol Chem*. 2000;275:9047–9054.
12. Hirosumi J, Tuncman G, Chang L, Gorgun CZ, Uysal KT, Maeda K, Karin M, Hotamisligil GS. A central role for JNK in obesity and insulin resistance. *Nature*. 2002;420:333–336.
13. Vernia S, Cavanagh-Kyros J, Garcia-Haro L, Sabio G, Barrett T, Jung DY, Kim JK, Xu J, Shulha HP, Garber M, Gao G, Davis RJ. The PPARalpha-FGF21 hormone axis contributes to metabolic regulation by the hepatic JNK signaling pathway. *Cell Metab*. 2014;20:512–525.
14. Tuncman G, Hirosumi J, Solinas G, Chang L, Karin M, Hotamisligil GS. Functional in vivo interactions between JNK1 and JNK2 isoforms in obesity and insulin resistance. *Proc Natl Acad Sci USA*. 2006;103:10741–10746.
15. Osto E, Matter CM, Kouroedov A, Malinski T, Bachschmid M, Camici GG, Kilic U, Stallmach T, Boren J, Iliceto S, Luscher TF, Cosentino F. c-Jun N-terminal kinase 2 deficiency protects against hypercholesterolemia-induced endothelial dysfunction and oxidative stress. *Circulation*. 2008;118:2073–2080.
16. Ricci R, Sumara G, Sumara I, Rozenberg I, Kurrer M, Akhmedov A, Hersberger M, Eriksson U, Eberli FR, Becher B, Boren J, Chen M, Cybulsky MI, Moore KJ, Freeman MW, Wagner EF, Matter CM, Luscher TF. Requirement of JNK2 for scavenger receptor A-mediated foam cell formation in atherogenesis. *Science*. 2004;306:1558–1561.
17. Park JH, Park M, Byun CJ, Jo I. c-Jun N-terminal kinase 2 phosphorylates endothelial nitric oxide synthase at serine 116 and regulates nitric oxide production. *Biochem Biophys Res Commun*. 2012;417:340–345.
18. Cho DH, Park JH, Joo Lee E, Jong Won K, Lee SH, Kim YH, Hwang S, Ja Kwon K, Young Shin C, Song KH, Jo I, Han SH. Valproic acid increases NO production via the SH-PTP1-CDK5-eNOS-Ser(116) signaling cascade in endothelial cells and mice. *Free Radic Biol Med*. 2014;76:96–106.
19. Sugita M, Sugita H, Kaneki M. Increased insulin receptor substrate 1 serine phosphorylation and stress-activated protein kinase/c-Jun N-terminal kinase activation associated with vascular insulin resistance in spontaneously hypertensive rats. *Hypertension*. 2004;44:484–489.
20. Bennett BL, Sasaki DT, Murray BW, O'Leary EC, Sakata ST, Xu W, Leisten JC, Motiwala A, Pierce S, Satoh Y, Bhagwat SS, Manning AM, Anderson DW. SP600125, an anthrapyrazolone inhibitor of Jun N-terminal kinase. *Proc Natl Acad Sci USA*. 2001;98:13681–13686.
21. Zhou MS, Schulman IH, Chadipiralla K, Raij L. Role of c-Jun N-terminal kinase in the regulation of vascular tone. *J Cardiovasc Pharmacol Ther*. 2010;15:78–83.
22. Bain J, McLauchlan H, Elliott M, Cohen P. The specificities of protein kinase inhibitors: an update. *Biochem J*. 2003;371:199–204.
23. Bain J, Plater L, Elliott M, Shpiro N, Hastie CJ, McLauchlan H, Klevernic I, Arthur JS, Alessi DR, Cohen P. The selectivity of protein kinase inhibitors: a further update. *Biochem J*. 2007;408:297–315.
24. Bonny C, Oberson A, Negri S, Sauser C, Schorderet DF. Cell-permeable peptide inhibitors of JNK: novel blockers of beta-cell death. *Diabetes*. 2001;50:77–82.
25. Kaneto H, Nakatani Y, Miyatsuka T, Kawamori D, Matsuoka TA, Matsuhisa M, Kajimoto Y, Ichijo H, Yamasaki Y, Hori M. Possible novel therapy for diabetes with cell-permeable JNK-inhibitory peptide. *Nat Med*. 2004;10:1128–1132.
26. Borsello T, Clarke PG, Hirt L, Vercelli A, Repici M, Schorderet DF, Bogousslavsky J, Bonny C. A peptide inhibitor of c-Jun N-terminal kinase protects against excitotoxicity and cerebral ischemia. *Nat Med*. 2003;9:1180–1186.
27. He B, Piao D, Yu C, Wang Y, Han P. Amelioration in hepatic insulin sensitivity by reduced hepatic lipid accumulation at short-term after Roux-en-Y gastric bypass surgery in type 2 diabetic rats. *Obes Surg*. 2013;23:2033–2041.
28. Zeng G, Nystrom FH, Ravichandran LV, Cong LN, Kirby M, Mostowski H, Quon MJ. Roles for insulin receptor, PI3-kinase, and Akt in insulin-signaling pathways related to production of nitric oxide in human vascular endothelial cells. *Circulation*. 2000;101:1539–1545.
29. Ding L, Zhang J. Glucagon-like peptide-1 activates endothelial nitric oxide synthase in human umbilical vein endothelial cells. *Acta Pharmacol Sin*. 2012;33:75–81.
30. Forstermann U, Munzel T. Endothelial nitric oxide synthase in vascular disease: from marvel to menace. *Circulation*. 2006;113:1708–1714.
31. Farah C, Kleindienst A, Bolea G, Meyer G, Gayrard S, Geny B, Obert P, Cazorla O, Tanguy S, Reboul C. Exercise-induced cardioprotection: a role for eNOS uncoupling and NO metabolites. *Basic Res Cardiol*. 2013;108:389.
32. Montecucco F, Steffens S, Mach F. Insulin resistance: a proinflammatory state mediated by lipid-induced signaling dysfunction and involved in atherosclerotic plaque instability. *Mediators Inflamm*. 2008;2008:767623.
33. Rask-Madsen C, King GL. Mechanisms of disease: endothelial dysfunction in insulin resistance and diabetes. *Nat Clin Pract Endocrinol Metab*. 2007;3:46–56.
34. Erdogdu O, Eriksson L, Xu H, Sjoholm A, Zhang Q, Nystrom T. Exendin-4 protects endothelial cells from lipoapoptosis by PKA, PI3K, eNOS, p38 MAPK, and JNK pathways. *J Mol Endocrinol*. 2013;50:229–241.
35. Salisbury D, Bronas U. Reactive oxygen and nitrogen species: impact on endothelial dysfunction. *Nurs Res*. 2015;64:53–66.
36. Son Y, Kim S, Chung HT, Pae HO. Reactive oxygen species in the activation of MAP kinases. *Methods Enzymol*. 2013;528:27–48.
37. Ferdaoussi M, Abdelli S, Yang JY, Cornu M, Niederhauser G, Favre D, Widmann C, Regazzi R, Thorens B, Waeber G, Abderrahmani A. Exendin-4 protects beta-cells from interleukin-1 beta-induced apoptosis by interfering with the c-Jun NH2-terminal kinase pathway. *Diabetes*. 2008;57:1205–1215.
38. Han L, Yu Y, Sun X, Wang B. Exendin-4 directly improves endothelial dysfunction in isolated aortas from obese rats through the CAMP or AMPK-eNOS pathways. *Diabetes Res Clin Pract*. 2012;97:453–460.
39. Erdogdu O, Nathanson D, Sjoholm A, Nystrom T, Zhang Q. Exendin-4 stimulates proliferation of human coronary artery endothelial cells through eNOS-, PKA- and PI3K/Akt-dependent pathways and requires GLP-1 receptor. *Mol Cell Endocrinol*. 2010;325:26–35.
40. Farb MG, Karki S, Park SY, Saggese SM, Carmine B, Hess DT, Apovian C, Fetterman JL, Breton-Romero R, Hamburg NM, Fuster JJ, Zuriaga MA, Walsh K, Gokce N. WNT5A-JNK regulation of vascular insulin resistance in human obesity. *Vasc Med*. 2016;21:489–496.
41. Breton-Romero R, Feng B, Holbrook M, Farb MG, Fetterman JL, Linder EA, Berk BD, Masaki N, Weisbrod RM, Inagaki E, Gokce N, Fuster JJ, Walsh K, Hamburg NM. Endothelial dysfunction in human diabetes is mediated by Wnt5a-JNK signaling. *Arterioscler Thromb Vasc Biol*. 2016;36:561–569.
42. Ijaz A, Tejada T, Catanuto P, Xia X, Elliot SJ, Lenz O, Jauregui A, Saenz MO, Molano RD, Pileggi A, Ricordi C, Fornoni A. Inhibition of c-Jun N-terminal kinase improves insulin sensitivity but worsens albuminuria in experimental diabetes. *Kidney Int*. 2009;75:381–388.
43. Yu G, Peng T, Feng Q, Tyml K. Abrupt reoxygenation of microvascular endothelial cells after hypoxia activates ERK1/2 and JNK1, leading to NADPH oxidase-dependent oxidant production. *Microcirculation*. 2007;14:125–136.
44. Spreckley E, Murphy KG. The L-cell in nutritional sensing and the regulation of appetite. *Front Nutr*. 2015;2:23.
45. Lim GE, Huang GJ, Flora N, LeRoith D, Rhodes CJ, Brubaker PL. Insulin regulates glucagon-like peptide-1 secretion from the enteroendocrine L cell. *Endocrinology*. 2009;150:580–591.
46. Cardozo AK, Buchillier V, Mathieu M, Chen J, Ortis F, Ladriere L, Allaman-Pillet N, Poirot O, Kellenberger S, Beckmann JS, Eizirik DL, Bonny C, Maurer F. Cell-permeable peptides induce dose- and length-dependent cytotoxic effects. *Biochem Biophys Acta*. 2007;1768:2222–2234.
47. Repici M, Mare L, Colombo A, Ploia C, Sclip A, Bonny C, Nicod P, Salmona M, Borsello T. c-Jun N-terminal kinase binding domain-dependent phosphorylation of mitogen-activated protein kinase kinase 4 and mitogen-activated protein kinase kinase 7 and balancing cross-talk between c-Jun N-terminal kinase and extracellular signal-regulated kinase pathways in cortical neurons. *Neuroscience*. 2009;159:94–103.

Supplemental Material

Data S1

Tissue harvesting and blood collection

Rats were sacrificed eight days after surgery and start of treatment. Rats were fasted overnight and sacrificed at the beginning of the light cycle by isoflurane anesthesia followed by heart exsanguination. For plasma analyses, blood collected in Microvette EDTA vacutainers was supplemented with a DPPIV inhibitor; for serum analyses, blood was collected in Microvette vacutainers. After centrifugation, plasma or serum were stored at -80°C. Organs were harvested within 30 minute after exsanguination. The thoracic aorta was placed immediately in cold modified Krebs-Ringer bicarbonate solution (pH 7.4, 37°C, 95% O2, 5% CO2) of the following composition (mmol/L): NaCl (118.6), KCl (4.7), CaCl2 (2.5), KH2PO4 (1.2), MgSO4 (1.2), NaHCO3 (25.1), glucose (11.1), and calcium EDTA (0.026). The aorta was cleaned from adhering connective tissue and was either snap-frozen in liquid nitrogen and stored at -80°C or used immediately for *ex vivo* organ chamber experiments.

Dihydroethidium staining on rat aortae

Frozen 10 µm sections from aortae were cut with a Leica CM3050S cryostat and placed on positive-charged slides Superfrost Plus. Dihydroethidium (DHE) was prepared as stock solution in DMSO, diluted in deoxygenated PBS (final concentration 5 µM), and applied to frozen sections for 30 min at 37°C. Nuclei were counterstained with Hoechst 33258 (final concentration 1µg/ml). Slides were coverslipped and images taken on a SP8 microscope (10x/0.30 objective; Leica, Solms, Germany), and quantified (ImageJ, NIH). DHE fluorescence was calculated

by subtracting the auto-fluorescence signal (green channel) from the DHE signal (red channel), and normalized to the total fluorescent area.

qPCR analysis

Expression of kidney injury molecule-1 (KIM-1) and lipocalin-2 (NGAL) was analyzed by qPCR of snap-frozen kidney tissue. RNA was isolated from frozen kidneys with a RNaeasy Mini Kit and reverse transcribed with a Ready-To-Go You-Prime First-Strand Beads. Rat-specific primers were used for KIM-1 (forward: GTGGGTCACCCTGTCACAAT, reverse: ATGTTGTATCGACCGCTGCT) and NGAL (forward: GATGAACTGAAGGAGCGATTC, reverse: TCGGTGGGAACAGAGAAAAC). CT results were normalized to GAPDH CT.

Histological analysis

Representative samples of aorta, liver, pancreas, kidneys, thyroid glands, inguinal white adipose tissue and interscapular brown adipose tissue were fixed in 10% neutral buffered formalin and embedded in paraffin. Sections (3-5 µm) were prepared, mounted on glass slides, deparaffinised in xylene, rehydrated through graded alcohols and stained with haematoxylin and eosin (H&E) for the histological examination. All slides were scanned using digital slide scanner NanoZoomer-XR C12000 (Hamamatsu, Hamamatsu City, Japan) and images were taken using NDP-view2 viewing software (Hamamatsu).

Renal injury, characterized by tubular degeneration and regeneration and interstitial inflammation, was assessed by light microscopy in a blinded fashion (by G.P.). A semi-quantitative scoring of 0-5 was employed, based on the proportion of affected tubules: 0, none; 1, <10% (slight injury); 2, 11-25% (mild); 3, 26-45% (moderate); 4, 46-75% (marked); and 5, >75% (severe).

Supplemental Results

JNK2 inhibition after *in vivo* SP600125 treatment induces protective vascular effects similar to RYGB

In the pilot experiment, eight-day treatment of DIO sham-operated *ad libitum*-fed rats with SP600125 increased endothelium-mediated relaxation in response to GLP-1 and insulin similar to RYGB, although the effect was less pronounced than in RYGB rats (Fig. S1E-F). *In vivo* SP600125 treatment decreased aortic JNK2 phosphorylation compared to controls$_{DMSO}$ rats, while JNK1 phosphorylation was not affected (Fig. S2A). JNK2 inhibition was followed by decreased IRS-1 Ser307 and increased Akt Ser473 phosphorylation and higher eNOS dimerization similar to RYGB and D-JNK treatment (Fig. S2B-E). Additionally, *in vivo* SP600125 treatment also decreased aortic superoxide anion levels and NADPH activity comparable to RYGB surgery (Fig. S5A-B). SP600125 did not affect circulating GLP-1 levels (Fig. S5C). These results support a direct role of vascular JNK2 inactivation in lowering oxidative stress and activating Akt/eNOS signaling pathways to improve endothelial function after RYGB, and prompted us to perform the main experiment using the more specific JNK inhibitor D-JNK.

Aortic eNOS Ser116 phosphorylation

It has been published that JNK2 directly inhibits eNOS by Ser116 phosphorylation in studies using bovine aortic endothelial cells [1] and mouse aortae [2]. Unfortunately, we could not detect eNOS Ser116 phosphorylation in rat aorta with the same anti-human Ser116 antibody used in previous publications [1, 2]. This antibody, which is the only commercially available anti-phospho-Ser 116 eNOS, showed bands between 100 kDa and 130 kDa, but not at 140 kDa, which is the expected molecular

weight of eNOS. In contrast, total eNOS was detected at 140 kDa (Fig. S3). The eNOS Ser116 antibody has not been validated in rat tissue before (personal communication; Merck Millipore) and the only available results had been obtained with bovine aortic endothelial cells [1]. One study assessed eNOS Ser116 in mice aortae, but representative images for total and phosphorylated eNOS did not report the molecular weight references to rule out an unspecific binding [2]. A sequence alignment of the human and rat immunogenic regions used for this antibody showed sub-optimal homology, suggesting limited reactivity (personal communication; Merck Millipore). Therefore, it is possible that the antibody is not suitable to detect eNOS Ser116 phosphorylation specifically in rat tissue.

D-TAT carrier peptide-dependent kidney toxicity

D-JNK treatment affected food intake and body weight similar to RYGB (Fig.6B-C), while SP600125 or D-JNK in chow-fed lean rats (Fig. S6A-C) had no effect. This prompted us to investigate organ toxicity as a potential cause of weight loss after chronic D-JNK treatment in obese rats. Circulating markers of liver and kidney damage were assessed (urea, creatinine, cystatin C, transferrin, albumin, alanine aminotransferase, aspartate aminotransferase, lactate dehydrogenase). Only creatinine and cystatin C levels were significantly elevated in the D-JNK group, suggesting potential kidney toxicity (Fig. S6D-E). Furthermore, histological analysis indicated tubular degeneration and necrosis, accompanied by tubular regeneration and interstitial, predominantly lymphohistiocytic cell infiltration (Fig. S7A-B). Renal injury also occurred in controls$_{D\text{-}TAT}$ rats but was more moderate (approximately 40% tubules affected) compared to D-JNK-treated rats (> 80%). These histological changes were accompanied by impaired kidney function in

controls$_{D\text{-}TAT}$ and D-JNK animals, with increased urinary excretion and a presumably compensatory higher water intake (Fig. S7C-F). There was no statistically significant difference in urine excretion and water intake between controls$_{D\text{-}TAT}$ and D-JNK animals. Gene expression analysis of acute kidney injury markers showed increased kidney injury molecule-1 (KIM-1) and neutrophil gelatinase-associated lipocalin/lipocalin 2 (NGAL) in obese rats upon D-JNK and D-TAT treatment (Fig. S7G-H). A slight increase of these kidney injury markers was also observed in chow-fed D-TAT- and D-JNK-treated animals while SP600125 did not affect KIM-1 and NGAL expression (Fig. S7G-H). The analyses of aorta, liver, pancreas, thyroid glands, white and brown adipose tissue from controls$_{D\text{-}TAT}$ and D-JNK rats did not show biochemical or histological signs of toxicity (data not shown), suggesting a kidney-specific effect. To our knowledge, this is the first study clearly showing *in vivo* D-JNK toxicity in the kidney. Published data on D-JNK pharmacokinetics after a single intra-peritoneal injection in mice reported a higher accumulation of D-JNK in the filter organs (kidney and liver) and in urine for up to one week, suggesting that D-JNK excretion is almost exclusively urinary [3]. In D-JNK, the active JNK inhibitory peptide is conjugated to a commonly used cell-penetrating oligo-peptide, the HIV-1 TAT protein, which functions as a carrier [4]. It has been reported that various cell-permeable peptides, including D-TAT oligo-peptides such as D-JNK, induce *in vitro* length-dependent cytotoxic effects irrespective of their sequence [5]. Therefore, the observed kidney damage was likely due to intrinsic cytotoxicity of the D-TAT carrier peptide independent of the D-JNK inhibitory activity [5]. This would explain why renal toxicity, which was observed in both controls$_{D\text{-}TAT}$ and D-JNK rats, was more pronounced in the D-JNK rats because of the peptide length. No toxicity was observed with SP600125, which supports the independence of toxicity from the JNK inhibitory activity of D-JNK.

Supplemental Figures

Figure S1

Concentration–response curves after 30 minute pre-incubation with 10^{-4} mol/L endothelial NO synthase inhibitor, L-NAME and submaximal contraction to NE in response to **(A)** GLP-1 and **(B)** insulin in $controls_{D\text{-}TAT}$, RYGB, and D-JNK rats (n=3 per group). Concentration–response curves after submaximal contraction to NE in response to **(C)** GLP-1 and **(D)** insulin in non-operated, chow-fed rats treated with D-TAT or D-JNK for eight days (n=2-4 per group). Relaxations in response to **(E)** GLP-1 and **(F)** insulin in RYGB, $controls_{DMSO}$, and SP600125 rats (*, **, *** p<0.05, p<0.01, p<0.001 RYGB vs. $controls_{DMSO}$, $^{\&\&, \&\&\&}$ p<0.01, p<0.001 RYGB vs. SP600125, as determined by two-way repeated measures ANOVA and Bonferroni post hoc test; n=5-10 per group). Results are shown as mean ± SD.

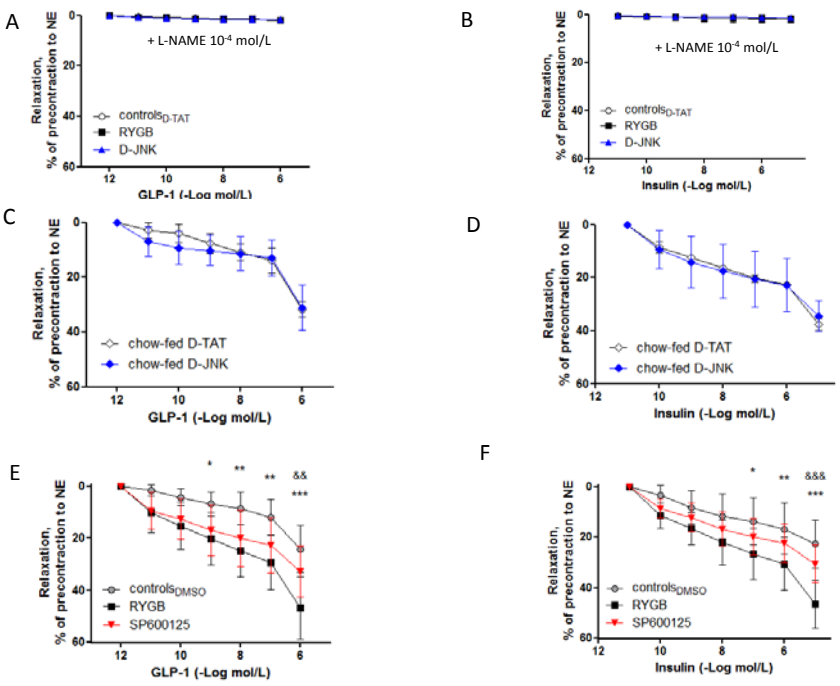

Fig. S1

Figure S2

Aortic **(A)** JNK1 and JNK2 phosphorylation, **(B)** IRS-1 Ser307, **(C)** Akt Ser473, **(D)** eNOS Ser1177 phosphorylation and **(E)** eNOS dimerization in $controls_{DMSO}$, RYGB, and SP600125 rats eight days after surgery/start of treatment. Representative Western blots and densitometric quantifications are shown (*, **, *** p<0.05, p<0.01, p<0.001 RYGB vs. $controls_{DMSO}$, §, §§ p<0.05, p<0.01 $controls_{DMSO}$ vs. SP600125, as determined by one-way ANOVA and Bonferroni *post hoc* test; n=5-11 per group). Results are shown as mean ± SD.

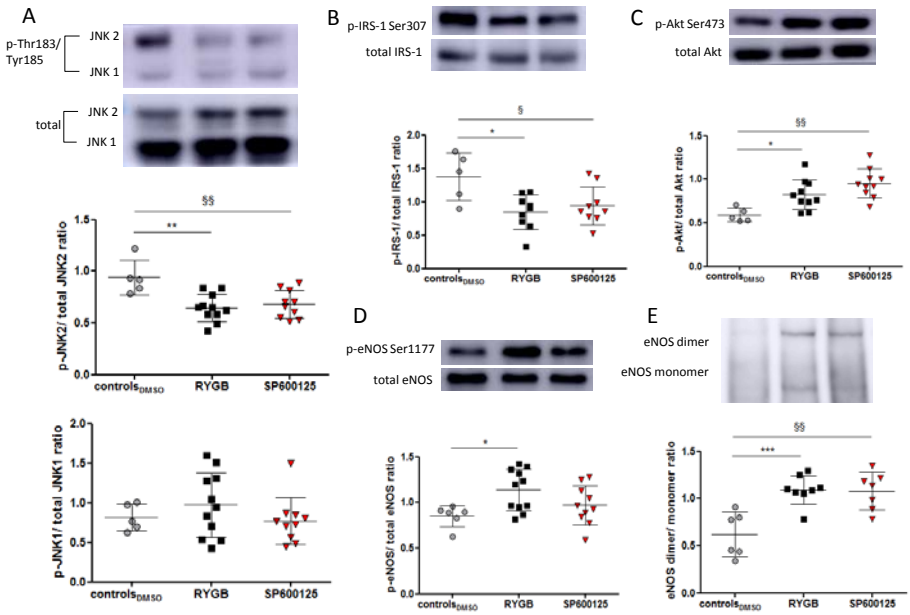

Fig. S2

Figure S3

Western blot analysis of **(A)** eNOS Ser116 phosphorylation and **(B)** total eNOS (molecular weight of 140 kDa) in the same aortic lysates from controls$_{D\text{-}TAT}$, RYGB, and D-JNK rats. Representative pictures are shown.

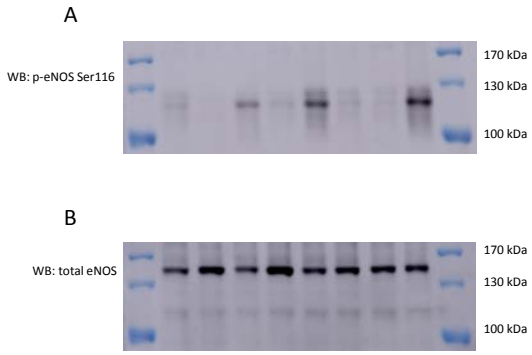

Fig. S3

Figure S4

Western blot analysis of phosphorylation of **(A)** PKC alpha/beta Thr638/641, **(B)** PKCβII Ser 660, **(C)** PKCδ Thr 505, **(D)** p38 MAPK Thr180/Tyr182, **(E)** ERK1/2 (44 and 42 KD, respectively) in controls$_{D\text{-}TAT}$, RYGB, and D-JNK rats eight days after surgery/start of treatment. Representative Western blots and densitometric quantifications are shown (* $p<0.05$ D-JNK vs RYGB and controls$_{D\text{-}TAT}$, as determined by one-way ANOVA and Bonferroni post hoc test; n=7 per group). Results are shown as mean ± SD.

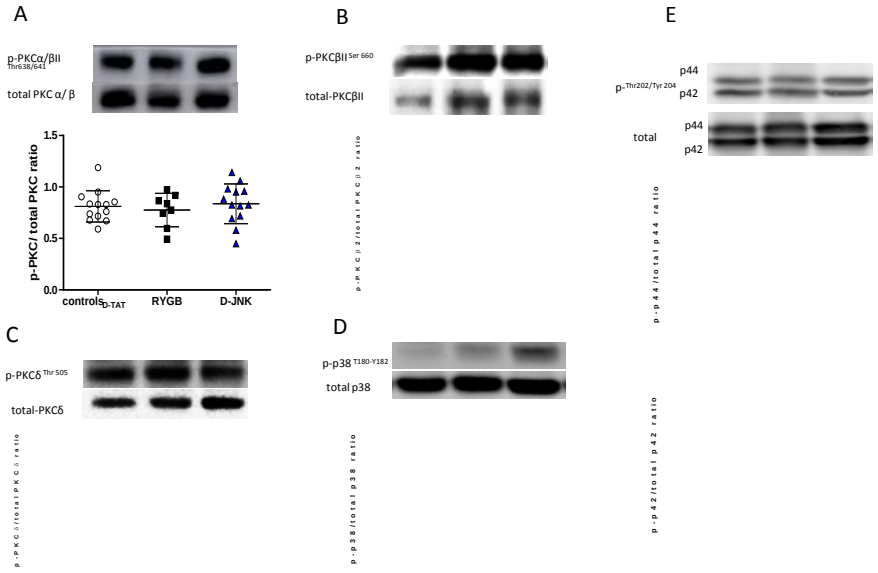

Fig. S4

Figure S5

(A) *In vitro* DHE fluorescent staining of anion superoxide and relative quantification in aortae isolated from $controls_{DMSO}$, RYGB and SP600125 rats eight days after surgery/start of treatment. Representative pictures are shown. **(B)** *In vitro* NADPH oxidase activity in aortae isolated eight days after surgery (* $p<0.05$ RYGB vs. all other groups, § $p<0.05$ $controls_{DMSO}$ vs. SP600125, as determined by one-way ANOVA and Bonferroni *post hoc* test; n=7-9 per group)**. (C)** Fasting plasma GLP-1 levels (* $p<0.05$ RYGB vs. all other groups, as determined by Kruskal-Wallis test and Dunn's Multiple Comparison test; n=6-16 per group). Results are shown as mean ± SD except in Figure S5C where results are presented as median ± IQR.

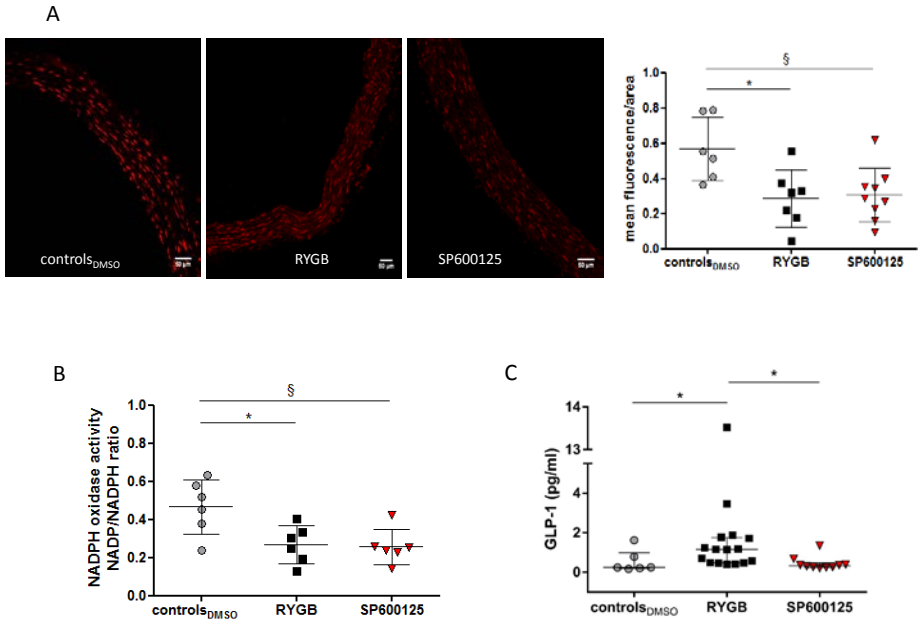

Fig. S5

Figure S6

(A) Cumulative 24-hour food intake (*, **, *** p<0.05, p<0.01, p<0.001 RYGB vs. $controls_{D\text{-}TAT}$, $controls_{DMSO}$, as determined by two-way ANOVA and Bonferroni *post hoc* test; n=8-13 per group) and **(B)** body weight of $controls_{DMSO}$, RYGB and SP600125 rats before and after surgery and start of treatment (day 0) (*, ** p<0.05, p<0.01 RYGB vs. $controls_{D\text{-}TAT}$, $controls_{DMSO}$, as determined by two-way repeated measures ANOVA and Bonferroni *post hoc* test; n=8-13 per group). **(C)** Body weight (n=4 per group) in non-operated, chow-fed rats treated with D-TAT or D-JNK for eight days (no differences, as determined by two-way repeated measures ANOVA and Bonferroni *post hoc* test; n=2-4 per group). **(D)** Serum creatinine and **(E)** plasma cystatin C levels in $controls_{D\text{-}TAT,}$ RYGB, and D-JNK rats eight days after surgery/start of treatment (** p<0.01 RYGB vs. D-JNK, ° p<0.05 controlsD-TAT vs. D-JNK, as determined by Kruskal-Wallis test and Dunn's Multiple Comparison test; n=6-8 per group). Results are shown as mean ± SD except in Figure S6D-E where results are presented as median ± IQR.

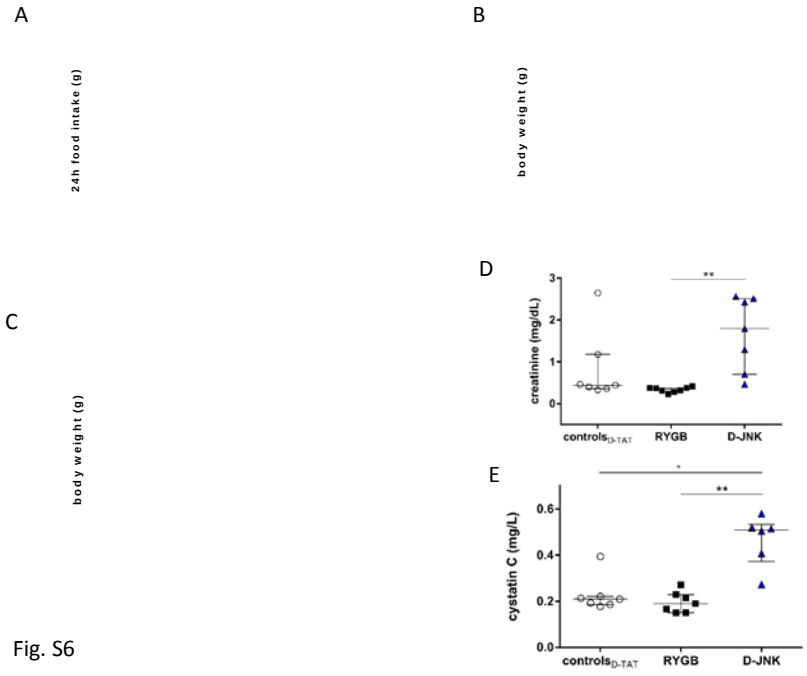

Fig. S6

Figure S7

Histological analysis by hematoxylin and eosin (H&E) staining of kidney from **(A)** a D-JNK and **(B)** a $controls_{D\text{-}TAT}$ rat euthanized eight days after sham surgery/start of treatment. Cumulative 24-hour urine excretion in **(C)** $controls_{D\text{-}TAT}$ rats and **(D)** D-JNK rats, and cumulative 24-hour water intake in **(E)** $controls_{D\text{-}TAT}$ rats and **(F)** D-JNK rats 1 day before and 7 and 8 days after surgery and start of treatment (#, ##, ### $p<0.05$, $p<0.01$, $p<0.001$ Day -1 vs. Day 7 and Day 8, as determined by one-way ANOVA and Bonferroni *post hoc* test; n=6 per group). qPCR analysis of kidney expression of **(G)** kidney injury molecule-1(KIM-1) and **(H)** neutrophil gelatinase-associated lipocalin (NGAL) eight days after surgery and start of treatment (°, °°° $p<0.05$, $p<0.001$ D-JNK vs. all other groups, as determined by Kruskal-Wallis test and Dunn's Multiple Comparison test; n=4-7 per group). Results are shown as mean ± SD except in Figure S7G-H where results are presented as median ± IQR.

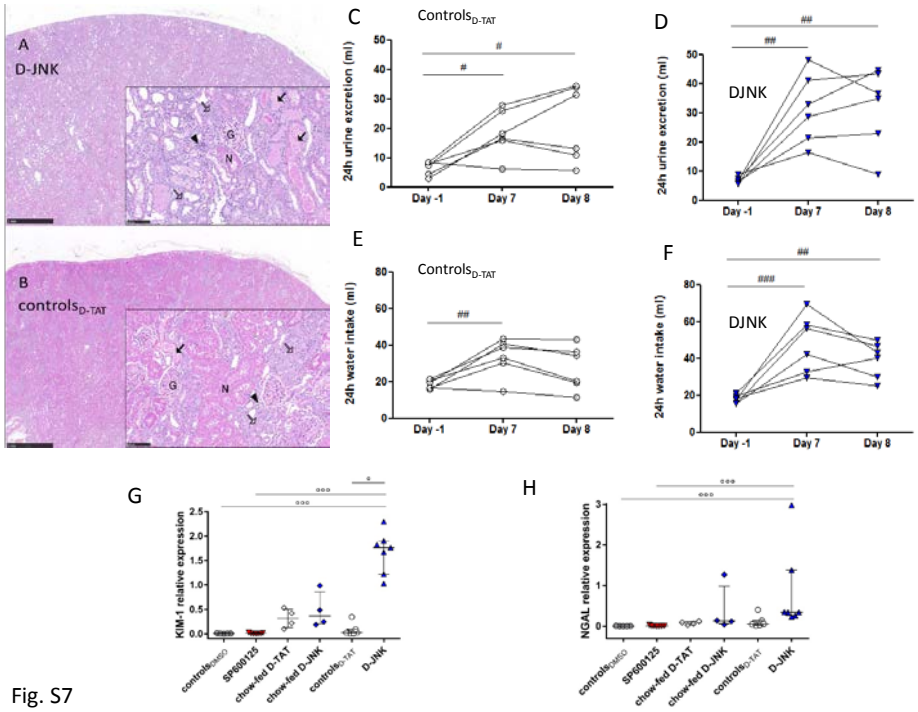

Fig. S7

Supplemental References

1. Park JH, Park M, Byun CJ, Jo I. C-jun n-terminal kinase 2 phosphorylates endothelial nitric oxide synthase at serine 116 and regulates nitric oxide production. *Biochemical and biophysical research communications*. 2012;417:340-345
2. Cho DH, Park JH, Joo Lee E, Jong Won K, Lee SH, Kim YH, Hwang S, Ja Kwon K, Young Shin C, Song KH, Jo I, Han SH. Valproic acid increases no production via the sh-ptp1-cdk5-enos-ser(116) signaling cascade in endothelial cells and mice. *Free radical biology & medicine*. 2014;76:96-106
3. Davoli E, Sclip A, Cecchi M, Cimini S, Carra A, Salmona M, Borsello T. Determination of tissue levels of a neuroprotectant drug: The cell permeable jnk inhibitor peptide. *Journal of pharmacological and toxicological methods*. 2014;70:55-61
4. Bonny C, Oberson A, Negri S, Sauser C, Schorderet DF. Cell-permeable peptide inhibitors of jnk: Novel blockers of beta-cell death. *Diabetes*. 2001;50:77-82
5. Cardozo AK, Buchillier V, Mathieu M, Chen J, Ortis F, Ladriere L, Allaman-Pillet N, Poirot O, Kellenberger S, Beckmann JS, Eizirik DL, Bonny C, Maurer F. Cell-permeable peptides induce dose- and length-dependent cytotoxic effects. *Biochimica et biophysica acta*. 2007;1768:2222-2234